Unveiling the redox-active character of imidazolin-2-thiones derived from amino-substituted N-Heterocyclic Carbenes

Mirko Ruamps, Stéphanie Bastin, Lionel Rechignat, Alix Sournia-Saquet, Dmitry A. Valyaev, Jean-Marie Mouesca, Noël Lugan, Vincent Maurel, Vincent César

Supporting Information

Contents

Materials and methods

All manipulations were performed under an inert atmosphere of dry nitrogen by using standard vacuum line and Schlenk tube techniques. Glassware was dried at 120°C in an oven for at least three hours. THF, diethyl ether, pentane, toluene and CH_2Cl_2 were dried using an Innovative Technology solvent purification system. Acetonitrile was dried over P_4O_{10} and subsequently distilled.

Imidazolium salts IMesHCl,[1] $IMes^{(NMe_2)}\cdot HOTf$,[2] and $IMes^{(NMe_2)_2}\cdot HOTf$,[2] were prepared according to literature procedures. 1,1'-diacetylferricinium tetrafluoroborate was prepared through oxidation of 1,1'-diacetylferrocene by benzoquinone/$HBF_4\cdot OEt_2$ according to a literature procedure.[3] The 0.5 M solution of KHMDS in toluene was prepared by weighing 2.0 g of solid KHMDS (stored in glovebox) in a volumetric flask and adding toluene to complete to 20 mL. $[NO](SbF_6)$ (Aldrich) was stored in the glovebox. All other reagents were commercially available and used as received.

NMR spectra were recorded on Bruker AV300 or AV400 spectrometers. Chemical shifts are reported in ppm (δ) compared to TMS (^1H and ^{13}C) using the residual peak of deuterated solvent as internal standard.[4] Elemental analyses were performed by the Microanalytical Service of the LCC and MS spectra (ESI mode) by the mass spectrometry service of the "Institut de Chimie de Toulouse".

Synthetic procedures

1,3-dimesityl-imidazolin-2-thione (1)

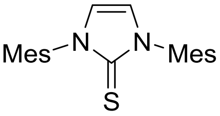

A solution of KHMDS (0.5 M in toluene, 2.2 mL, 1.1 mmol, 1.1 equiv.) was added dropwise to a solution of IMes·HCl (340.9 mg, 1.0 mmol) in THF (20 mL) at 0°C. After 30 min, elemental sulfur (38.5 mg, 1.2 mmol, 1.2 equiv.) was added as a solid and the solution was slowly warmed up overnight. After evaporation of volatiles, the crude product was purified by column chromatography (SiO_2, hexane/EtOAc : 4/1) to give an off-white powder (310 mg, 92%). ^1H NMR (400 MHz, $CDCl_3$): δ = 7.02 (s, 4H, CH_{Mes}), 6.80 (s, 2H, CH_{Im}), 2.35 (s, 6H, $CH_{3\ \text{para}}$), 2.16 (s, 12H, $CH_{3\ \text{ortho}}$). $^{13}C\{^1H\}$ NMR (101 MHz, $CDCl_3$): δ = 163.5 ($N_2C{=}S$), 139.3, 135.7, 133.7 (C_{Ar}), 129.3 (CH_{Mes}), 118.1 (CH_{Im}), 21.3 ($CH_{3\ \text{para}}$), 18.0 ($CH_{3\ \text{ortho}}$). MS (ESI, positive mode): m/z (%): 337 (100) $[M + H]^+$. Elemental analysis *calcd* (%) for $C_{21}H_{24}N_2S$ (MW = 336.50) + 0.05 CH_2Cl_2: C 74.2, H 7.1, N 8.2; *found*: C 74.2, H 6.8, N 8.2.

---

[1] L. Hintermann, *Beilstein J. Org. Chem.*, 2007, **3**, 22.

[2] Y. Zhang, V. César, G. Storch, N. Lugan and G. Lavigne, *Angew. Chem. Int. Ed.*, 2014, **53**, 6482.

[3] C. Guillon and P. Vierling, *J. Organomet. Chem.* 1994, **464**, C42.

[4] G. R. Fulmer, A. J. M. Miller, N. H. Sherden, H. E. Gottlieb, A. Nudelman, B. M. Stoltz, J. E. Bercaw and K. I. Goldberg, *Organometallics,* 2010, **29**, 2176.

1,3-dimesityl-4-(dimethylamino)imidazolin-2-thione ($\mathbf{1^{NMe_2}}$)

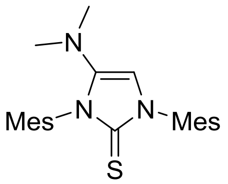

A solution of KHMDS (0.5 M in toluene, 1.1 mL, 0.55 mmol, 1.1 equiv.) was added dropwise to a solution of IMes$^{(NMe_2)}$·HOTf (249 mg, 0.5 mmol) in THF (10 mL) at 0°C. After 30 min, elemental sulfur (24 mg, 0.75 mmol, 1.5 equiv.) was added as a solid and the solution was slowly warmed up overnight. After evaporation of the volatiles, the crude residue was purified by column chromatography (SiO_2, petroleum ether/EtOAc: 8/1) to yield a white powder (165 mg, 87%). ^{1}H NMR (400 MHz, $CDCl_3$): δ = 7.00 (s, 2H, CH_{Mes}), 6.98 (s, 2H, CH_{Mes}), 6.09 (s, 1H, CH_{Im}), 2.49 (s, 6H, $N(CH_3)_2$), 2.33 (s, 3H, $CH_{3\,para}$), 2.32 (s, 3H, $CH_{3\,para}$), 2.17 (s, 6H, $CH_{3\,ortho}$), 2.16 (s, 6H, $CH_{3\,ortho}$). $^{13}C\{^1H\}$ NMR (101 MHz, $CDCl_3$): δ = 160.7 (N_2C=S), 142.5, 139.1, 138.9, 136.4, 135.8, 134.0, 132.3 (C_{Ar}), 129.5, 129.2 (CH_{Mes}), 101.8 (CH_{Im}), 42.9 ($N(CH_3)_2$), 21.4, 21.3 ($CH_{3\,para}$), 18.3, 18.0 ($CH_{3\,ortho}$). MS (ESI, positive mode): m/z (%): 380 (100) $[M + H]^+$. Elemental analysis *calcd* (%) for $C_{23}H_{29}N_3S$ (MW = 379.57): C 72.8, H 7.7, N 11.1; *found*: C 72.7, H 7.5, N 11.0.

1,3-dimesityl-4,5-bis(dimethylamino)imidazolin-2-thione ($\mathbf{1^{(NMe_2)_2}}$)

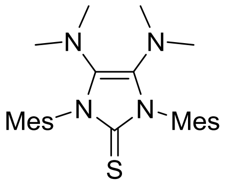

A solution of KHMDS (0.5 M in toluene, 1 mL, 0.5 mmol, 1.1 equiv.) was added dropwise to a solution of IMes$^{(NMe_2)_2}$·HOTf (248 mg, 0.45 mmol) in THF (20 mL) at – 80°C. After 30 min, elemental sulfur (22 mg, 0.66 mmol, 1.5 equiv.) was added as a solid and the solution was allowed to warm up to room temperature. All volatiles were evacuated *in vacuo* and the crude mixture was purified by column chromatography (SiO_2, hexane/EtOAc : 4/1) to give a white powder (122 mg, 63%). Single crystals suitable for an X-Ray diffraction experiment were grown by slow evaporation of a saturated solution of $\mathbf{1^{(NMe_2)_2}}$ in CH_2Cl_2. ^{1}H NMR (400 MHz, $CDCl_3$): δ = 6.97 (s, 4H, CH_{Mes}), 2.59 (s, 12H, $N(CH_3)_2$), 2.32 (s, 6H, $CH_{3\,para}$), 2.17 (s, 12H, $CH_{3\,ortho}$). $^{13}C\{^1H\}$ NMR (101 MHz, $CDCl_3$): δ = 157.6 (N_2C=S), 138.7, 136.4, 132.4, 131.0 (C_{Ar}), 129.3 (CH_{Mes}), 43.7 ($N(CH_3)_2$), 21.4 ($CH_{3\,para}$), 18.4 ($CH_{3\,ortho}$); MS (ESI, positive mode): m/z (%): 423 (100) $[M + H]^+$; HRMS (ESI): *m/z*: calcd. for $C_{25}H_{35}N_4S$: 423.2582; found: 423.2586, ε_r = 0.9 ppm; Elemental analysis *calcd* (%) for $C_{25}H_{34}N_4S$ (MW = 422.64): C 71.05, H 8.1, N 13.2; *found*: C 70.9, H 8.1, N 12.9.

Generation and EPR characterization of $[\mathbf{1^{NMe_2}}]^{\cdot+}$

Solid 1,1'-diacetylferricinium tetrafluoroborate (4.3 mg, 12 μmol, 1.0 equiv.) was added to a solution of $\mathbf{1^{NMe_2}}$ (4.55 mg, 12 μmol, 1.0 equiv.) in CH_2Cl_2 (1 mL) at – 40°C. After 5 min, 50 μL of the reaction mixture were syringed in an EPR tube, which was completed with 50 μL of toluene. The EPR spectra were immediately recorded.

Synthesis and isolation of $[\mathbf{1}^{(\mathrm{NMe_2})_2}]^{\cdot+}$

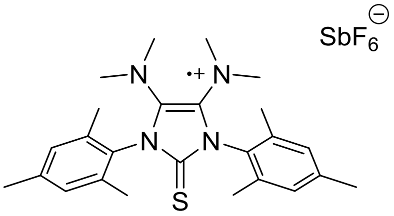

In a glove box, solid [NO](SbF_6) (34 mg, 0.128 mmol) was added all at once to a solution of thiourea $\mathbf{1}^{(\mathrm{NMe_2})_2}$ (59 mg, 0.139 mmol, 1.08 equiv.) in CH_2Cl_2 (2 mL). The solution color changed immediately from colorless to dark violet. After 5 min, the reaction mixture was layered with Et_2O and placed into the deep freezer at -30°C. After 3 days, the dark violet microcrystalline solid was filtered and dried under vacuum to give the pure title compound (75 mg, 89%). Elemental analysis *calcd* (%) for $C_{25}H_{34}F_6N_4SSb$ (MW = 658.39): C 45.6, H 5.2, N 8.5; *found*: C 45.5, H 5.0, N 8.25. UV−vis (CH_2Cl_2, λ_{max}, nm (ε, M^{-1} cm^{-1})): 227 (23460), 324 (9700), 370 (12800), 580 (6400).

Generation of $[\mathbf{1}^{(\mathrm{NMe_2})_2}](\mathbf{SbF_6})_2$

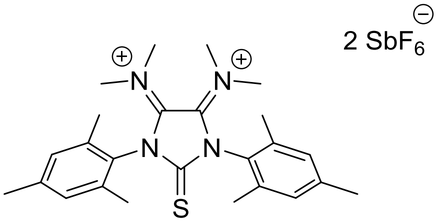

At – 20°C, the thiourea $\mathbf{1}^{(\mathrm{NMe_2})_2}$ (13.0 mg, 30.7 µmol) was added as a solid to a solution of [NO](SbF_6) (22 mg, 83 µmol, 2.7 equiv.) in CD_3CN (0.7 mL). The mixture immediately turned to dark orange and was stirred for additional 30 min at that temperature. The cooling bath was removed and the solution was cannulated into a NMR tube and the NMR spectra were recorded. Single crystals suitable for an X-Ray diffraction experiment were grown by layering Et_2O onto a solution of $[\mathbf{1}^{(\mathrm{NMe_2})_2}](\mathbf{SbF_6})_2$ in CH_2Cl_2 and a few drops of CH_3CN (to allow complete dissolution). ^1H NMR (400 MHz, CD_3CN): δ = 7.20 (s, 4H, C*H* $_{\mathrm{Mes}}$), 3.85 (s, 6H, N(C*H*$_3$)$_2$), 3.12 (s, 6H, N(C*H*$_3$)$_2$), 2.38 (s, 6H, C*H*$_3$ $_{\mathrm{para}}$), 2.25 (s, 12H, C*H*$_3$ $_{\mathrm{ortho}}$). $^{13}C\{^1H\}$ NMR (101 MHz, CD_3CN): δ = 170.7 (N_2*C*=S), 155.2 (*C*=NMe_2), 144.6, 137.3 (*C*$_{\mathrm{Mes}}$), 131.3 (*C*H $_{\mathrm{Mes}}$), 129.8 (*C*$_{\mathrm{Mes}}$), 51.0 (N(*C*H$_3$)$_2$), 48.1 (N(*C*H$_3$)$_2$), 21.2 (*C*H$_3$ $_{\mathrm{para}}$), 18.5 (*C*H$_3$ $_{\mathrm{ortho}}$).

X-Ray Crystallography

Data were collected on a Bruker D8/APEX II/Incoatec IµS Microsource diffractometer. All calculations were performed on a PC compatible computer using the WinGX system.[5] Full crystallographic data are given in Table S1. The structures were solved using the SIR92 program,[6] which revealed in each instance the position of most of the non-hydrogen atoms. All the remaining non-hydrogen atoms were located by the usual combination of full matrix least-squares refinement and difference electron density syntheses using the SHELX program.[7] Compound [**2**]SbF_6.Et_2O crystallizes as three independent motives per unit cell. Atomic scattering factors were taken from

---

[5] L. J. Farrugia, *J. Appl. Crystallogr.*, 1999, **32**, 837-838.

[6] A. Altomare, G. Cascarano, C. Giacovazzo and A. Guagliardi, *J. Appl. Crystallogr.*, 1994, **27**, 435-436.

[7] G. M. Sheldrick, *Acta Crystallogr.*, 2015, **C71**, 3-4.

the usual tabulations. Anomalous dispersion terms for the Sb and S atoms were included in Fc. All non-hydrogen atoms were allowed to vibrate anisotropically. The hydrogen atoms were generally set in idealized positions (R_3CH, C–H = 0.96 Å; R_2CH_2, C–H = 0.97 Å; RCH_3, C–H = 0.98 Å; C(sp^2)–H = 0.93 Å; U_{iso} 1.2 or 1.5 times greater than the U_{eq} of the carbon atom to which the hydrogen atom is attached) and their positions refined as "riding" atoms. CCDC 1843369-1843370 contain the supplementary crystallographic data for the two structures unveiled in this paper. These data can be obtained free of charge from the Cambridge Crystallographic Data Centre via www.ccdc.cam.ac.uk/data_request/cif

Electrochemical studies

Cyclic voltammetric measurements were carried out with a Autolab PGSTAT100 potentiostat controlled by GPES 4.09 software. Experiments were performed under argon at room temperature in a homemade airtight three-electrode cell. The reference electrode consisted of a saturated calomel electrode (SCE) separated from the solution by a glass frit. The counter electrode was a platinum wire of ca. 1 cm^2 apparent surface. The working electrode was a Pt microdisk (0.5 mm diameter). The supporting electrolyte, $(nBu_4N)(PF_6)$ (99% electrochemical grade), was dried at 120 °C and stored under Ar. The CH_2Cl_2 solutions of **1**, $\mathbf{1^{NMe2}}$, $\mathbf{1^{(NMe2)2}}$ used for the electrochemical studies were typically 10^{-3} M in complex and 0.1 M in supporting electrolyte. Before each measurement, the solutions were degassed by bubbling Ar and the working electrode was polished with a polishing machine. Potentials are referenced to the SCE, and were calibrated using the Fc/Fc^+ couple by adding ferrocene (10^{-3} M) at the end of the experiments. Under the experimental conditions employed in this work, the half-wave potential ($E_{1/2}$) of the Fc^+/Fc couple in CH_2Cl_2 occurred at $E_{1/2}$ = 0.46 V *vs.* SCE.

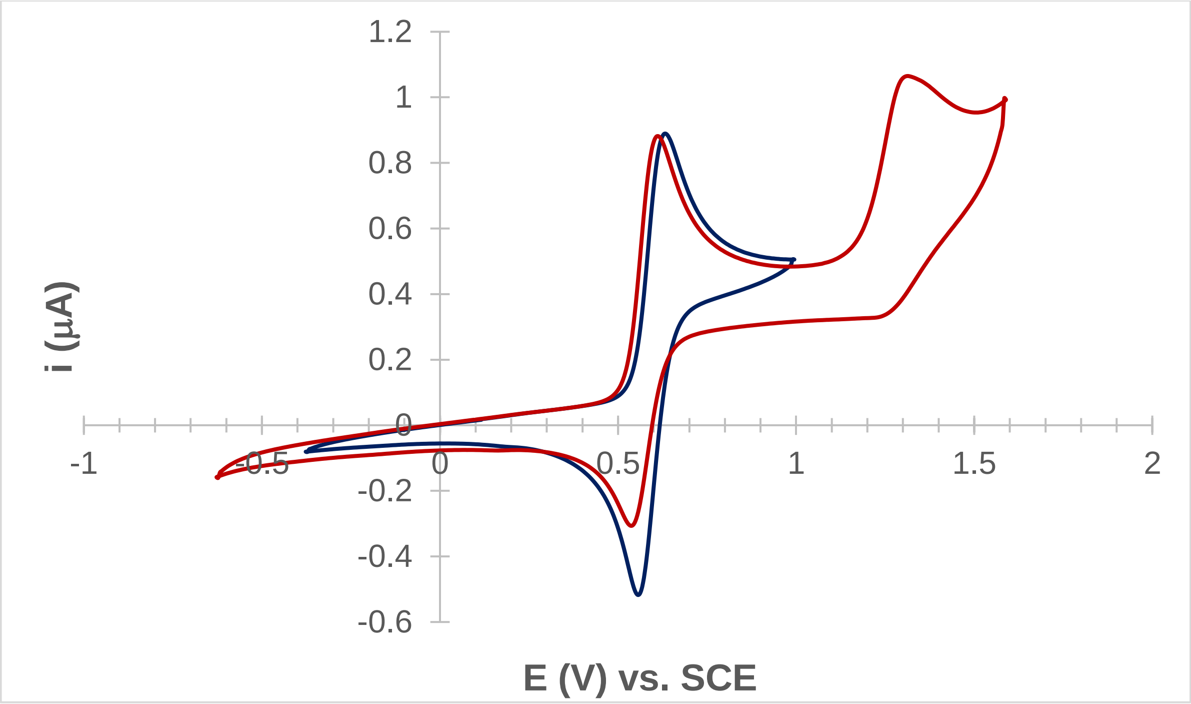

Figure S1: CV curves of [IMes$^{(NMe2)}$]=S (**1**$^{\mathbf{NMe2}}$) using different potential ranges. Conditions: 10^{-3} M in CH_2Cl_2, 0.1 M of $TBAPF_6$, scan rate = 200 mV.s^{-1}, working electrode = Pt).

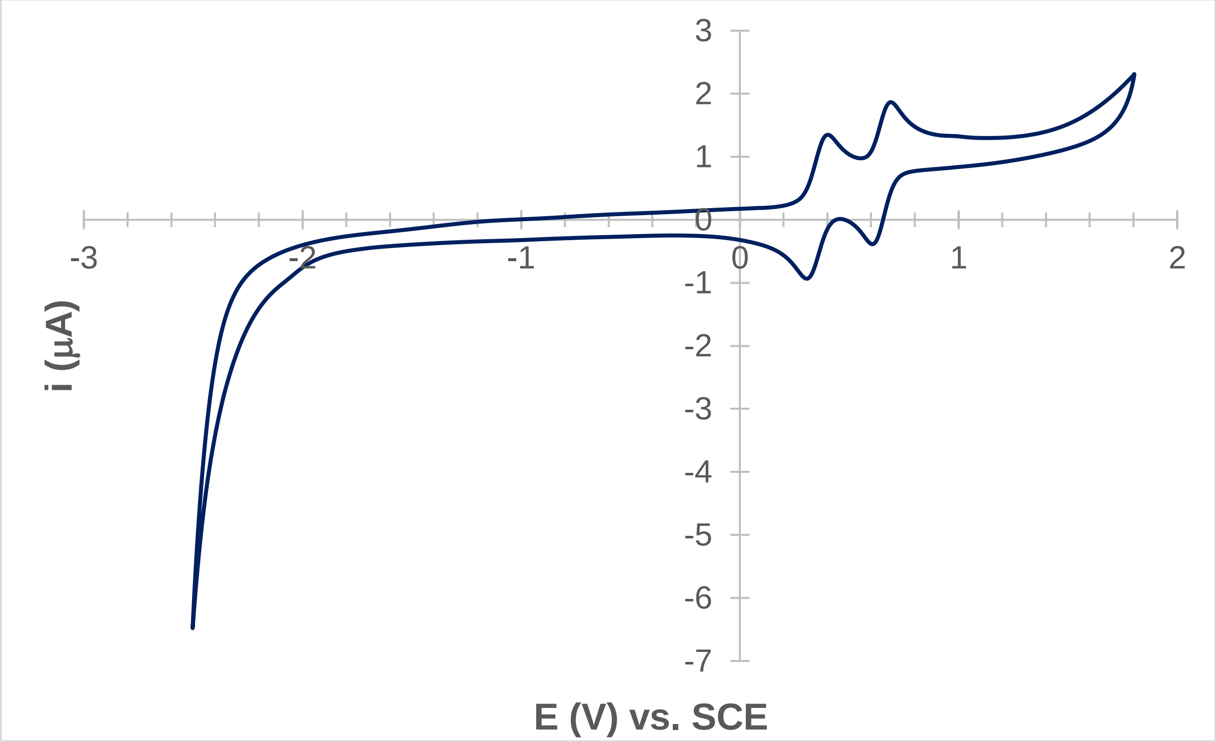

Figure S2: Full CV plot of [IMes$^{(NMe_2)_2}$=S] (**1**$^{\mathbf{(NMe_2)_2}}$). Conditions: 10^{-3} M in CH_2Cl_2, 0.1 M of $TBAPF_6$, scan rate = 200 mV.s^{-1}, working electrode = Pt).

EPR spectroscopy

X-Band EPR data were recorded using Elexsys ESP 500 and EMX Brüker EPR spectrometers. Spectra shown in the Figure 3 were recorded at room temperature using a microwave power of 2 mW, across a sweep width of 140 G, with a modulation amplitude of 0.2 G for $[\mathbf{1}^{\mathbf{NMe_2}}]^{\bullet+}$ and 1 G for $[\mathbf{1}^{\mathbf{(NMe_2)_2}}]^{\bullet+}$. Spectra recorded with lower modulation amplitudes for both species did not revealed more lines or different patterns (data not shown). Landé factors were measured by comparison with a reference DPPH sample (g = 2.0036). The numerical simulation of EPR spectra was done using EasySpin software (see ref. 15 in the main text).

To compute hfc's, we converged electronically both $[\mathbf{1}^{\mathbf{NMe_2}}]^{\bullet+}$ and $[\mathbf{1}^{\mathbf{(NMe_2)_2}}]^{\bullet+}$ radicals using TZ2P basis sets (frozen core option) and B3LYP[8] exchange-correlation potential.

nucleus	**DFT computation**	**EPR simulation**
H, C_5-H	40.7	36
3H, CH_3 (pointing to C_5 side)	13	12
3H, CH_3 (pointing to mesityl)	21.9	17.6
2N, $N(CH_3)_2$	20.2	15.8
N, N_1CN_3	5	3,7
N, N_1CN_3	3.9	3.7

Table S1: Hyperfine coupling constants (in MHz) obtained by DFT calculations and by numerical simulation of the EPR spectrum for the radical $[\mathbf{1}^{\mathbf{NMe_2}}]^{\bullet+}$.

---

[8] A. D. Becke, *J. Chem. Phys.* 1993, **98**, 1372-1377;

UV/Visible spectroscopy

The UV-vis spectra were recorded at room temperature on a Perkin-Elmer Lambda 950 spectrometer using a 1cm-path quartz cell with Teflon stopper.

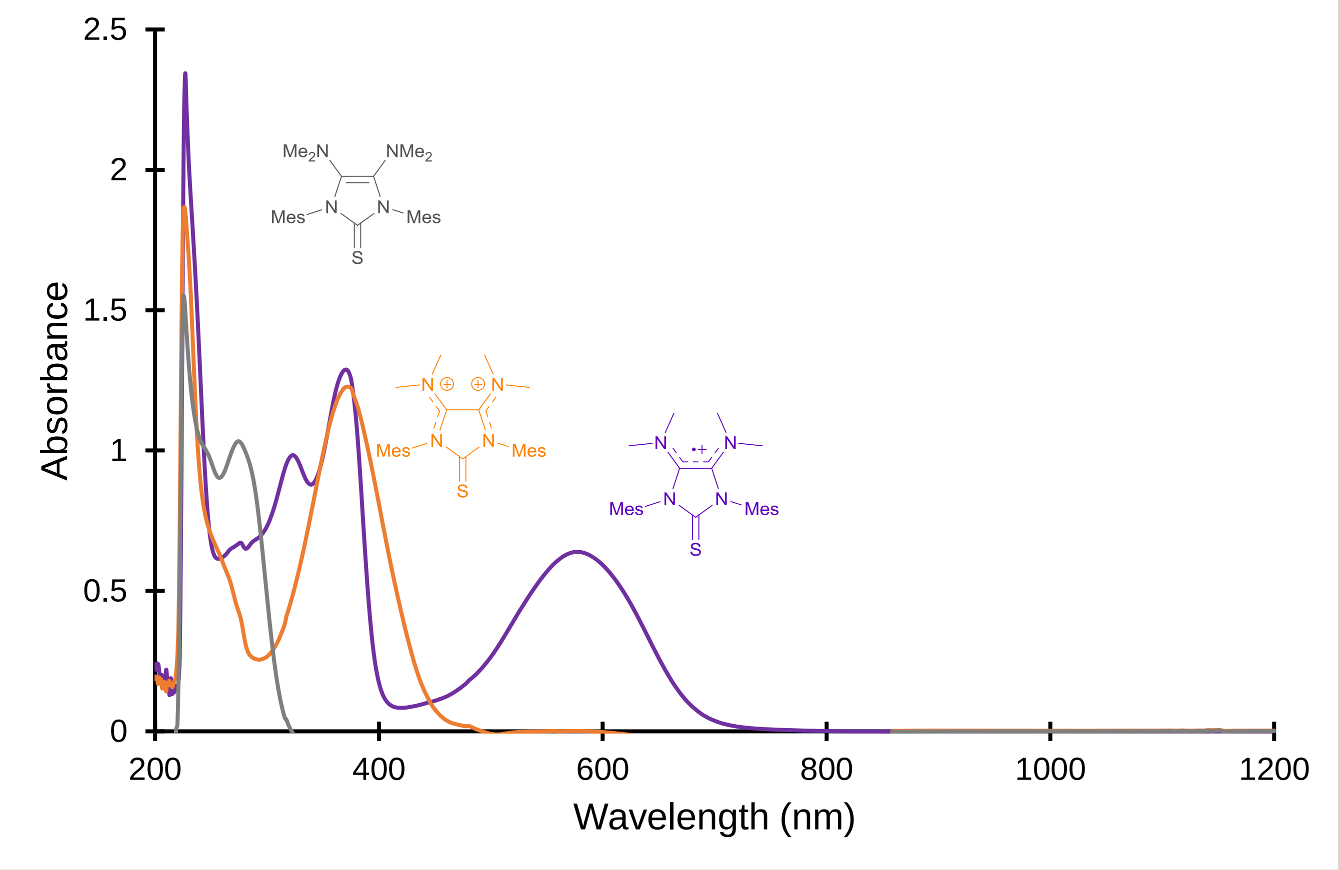

Figure S3: Normalized UV-visible spectra of compounds [**1**$^{(NMe_2)_2}$] (grey line), [**1**$^{(NMe_2)_2}$](SbF_6) (purple line) and [**1**$^{(NMe_2)_2}$]$(SbF_6)_2$ (orange line) (concentrations fixed at 10^{-4} M) recorded in CH_2Cl_2.

DFT calculations

All DFT calculations were performed with the ADF (Amsterdam Density Functional) code developed by E. J. Baerends and co-workers[9] using triple-zeta (TZ2P) basis sets (no frozen core).

Geometry optimizations of all species were performed relying on the Generalized Gradient Approximation (GGA) VBP exchange-correlation (XC) potential (VWN + BP: Vosko, Wilk & Nusair[10] + corrective terms by Becke[11] for the exchange, and Perdew[12] for the correlation) with ADF grid precision 6 throughout. The appropriate solvent environments (acetonitrile *versus* dichloromethane) have been modeled with the COSMO (COnductor-like Screening MOdel)[13] ADF module, representing the solvent as a dielectric continuum (ADF option: solv name), thus mimicking an average reaction field response of the environment.

Specific conditions for spectroscopic calculations (hfc's, g-tensors, NMR chemical shifts) are declined below.

---

[9] G. T. Velde and E. J. Baerends, *J. Comput. Phys.*, 1992, **99**, 84.

[10] S. H. Vosko, L. Wilk and M. Nusair, *Can. J. Phys.*, 1980, **58**, 1200.

[11] A. D. Becke, *Phys. Rev A*, 1988, **38**, 3098.

[12] J. P. Perdew, *Phys. Rev. B*, 1986, **33**, 8822.

[13] (a) A. Klamt and G. Schürmann, *J. Chem. Soc. Perkin Trans. 2,* 1993, 799; (b) A. Klamt, *J. Phys. Chem.*, 1995, **99**, 2224; (c) A. Klamt and V. Jona, *J. Chem. Phys.*, 1996, **105**, 9972.

Table S2: Geometrical features concerning [IMes$^{(NMe2)2}$)=S]

Method: DFT (SCM-ADF code), VBP (GGA) exchange-correlation potential, TZ2P basis sets

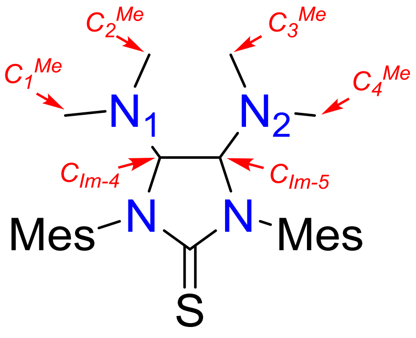 **Compound**	**angles (deg)** C_1^{Me}-N_1-C_2^{Me} C_3^{Me}-N_2-C_4^{Me}	**angles (deg)** C_1^{Me}-N_1-C_{Im-4} C_2^{Me}-N_1-C_{Im-4} C_3^{Me}-N_2-C_{Im-5} C_4^{Me}-N_2-C_{Im-5}	**Average sum** Σ_N **(deg)**	**bond lengths (Å)** C_{Im-4}-N_1 C_{Im-4}-N_1	**bond lengths (Å)** C_{Im-4}-C_{Im-5}	**Dihedral angles (deg)** C_1^{Me}-N_1-C_{Im-4}-C_{Im-5} C_3^{Me}-N_2-C_{Im-5}-C_{Im-4} C_2^{Me}-N_1-C_{Im-4}-C_{Im-5} C_4^{Me}-N_2-C_{Im-5}-C_{Im-4}
1$^{(NMe2)2}$	113.8	118.8	350.0$^{(a)}$	1.39	1.38	-41.7
		117.5				-41.0
	113.9	118.6				102.3
		117.5				101.9
[**1**$^{(NMe2)2}$]$^{\cdot+}$	114.4	121.3	359.6	1.35	1.43	-37.6
		123.9				-37.5
	114.4	121.1				150.6
		124.0				150.9
[**1**$^{(NMe2)2}$]$^{2+}$	112.6	122.7	359.4	1.32	1.50	-25.3
		124.1				-24.5
	112.7	122.8				163.6
		123.9				164.5

(a) Using neutral NMe_3 as a reference for pyramidalized nitrogen atom (Σ_N = 334.2°), the two nitrogen atoms in neutral **1**$^{(NMe2)2}$ are 39% sp^3 hybridized (i.e. 1.0-(350.0-334.1)/(360.0-334.2)).

Computation of the g-tensors

To compute g-tensors, we converged electronically both $[\mathbf{1}^{\mathbf{NMe_2}}]^{\bullet+}$ and $[\mathbf{1}^{\mathbf{(NMe_2)_2}}]^{\bullet+}$ radicals using the scalar relativistic approximation as a starting point for the separate EPR/NMR module (TZ2P basis sets and GGA exchange-correlation potential). This was performed taking into account the solvent (via the COSMO module, with parameter “solv” set to “dichloromethane”) as this was the determining factor. Other factors, such as larger basis sets (QZ4P), alternative XC potentials (SAOP or B3LYP), or full relativistic (i.e. spin-orbit) calculations, did not improve as much the calculations as solvation effects.

Experimentally, we measured:

for $[\mathbf{1}^{\mathbf{NMe_2}}]^{\bullet+}$: $g_1 = 2.0084$

for $[\mathbf{1}^{\mathbf{(NMe_2)_2}}]^{\bullet+}$: $g_2 = 2.0068$

Computationally:

for $[\mathbf{1}^{\mathbf{NMe_2}}]^{\bullet+}$: $g_1(\mathrm{GGA}) = 2.0115$

for $[\mathbf{1}^{\mathbf{(NMe_2)_2}}]^{\bullet+}$: $g_2(\mathrm{GGA})= 2.0080$

(without solvent: $g_1(\mathrm{GGA}) = 2.0168$ and $g_2(\mathrm{GGA}) = 2.0120$).

Though slightly larger in magnitude, the computed values reproduce well the experimental trend (g1 > g2), related to the fact that the spin population on the sulfur atom (i.e. the atom here with the largest spin-orbital coupling) is significantly larger in the $[\mathbf{1}^{\mathbf{NMe_2}}]^{\bullet+}$species (0.316) than in $[\mathbf{1}^{\mathbf{(NMe_2)_2}}]^{\bullet+}$species (0.227).

TD-DFT calculations on the UV-Vis spectrum of $[\mathbf{1}^{\mathbf{(NMe2)2}}](\mathbf{SbF_6})$

The first 50 singlet-singlet transitions and corresponding oscillator strengths have been computed by TD-DFT calculations (GGA-VBP potential, *in vacuo*) for the previously geometry-optimized $[\mathbf{1}^{\mathbf{(NMe2)2}}]^{\bullet+}$ species for which, experimentally, three absorption lines have been measured above 300 nm: 323 nm and 369 nm (near UV) and 578 nm (visible).

Computationally, three transitions exhibit the largest oscillator strength, one at 313 nm (f = 0.067 a.u.), the next one at 359 nm (f = 0.067 a.u.) and the last one at 582 nm (f = 0.089 a.u.). The spin α HOMO-LUMO gap implicates the orbitals 114 (occupied) and 115 (empty), respectively (occupied 113 and empty 114 for spin β). The orbital 114 is thus the SOMO (see Scheme below).

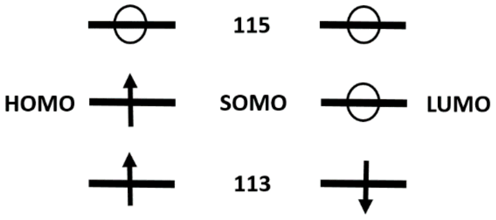

The main results are given in the following table.

Exp.(nm)	DFT			
	(nm)	f (a.u.)	Transition(s)	weight (%)
323	313	0.067	103β → 114β 114α → 120α	39 % 36 %
369	359	0.067	114α → 115α	76 %
578	**582**	**0.089**	**109β → 114β**	**78 %**

Table S3. Experimental and computed transitions (nm), oscillator strengths f (a.u.) and description of the main orbitals involved (with weights in %) for compound **$[1^{(NMe_2)_2}](SbF_6)$.**

The orbitals involved in the transitions are represented in figure S4.

The transition at 582 nm is made from the following transition: 109β → LUMO 114β (weight = 78 %).

The intermediary transition computed at 359 nm corresponds to the (spin α) HOMO → LUMO gap (114α → 115α) of weight 76 %. This 114α orbital becoming empty in the di-oxidized (2+) species, the fact of observing in the latter case a line at 372 nm (close to 359 nm for the 1+ species) is coincidental.

As for the transition computed at 313 nm (measured at 323 nm), it is made of two major contributions: 103β → 114β (39 %) and 114α → 120α (36 %).

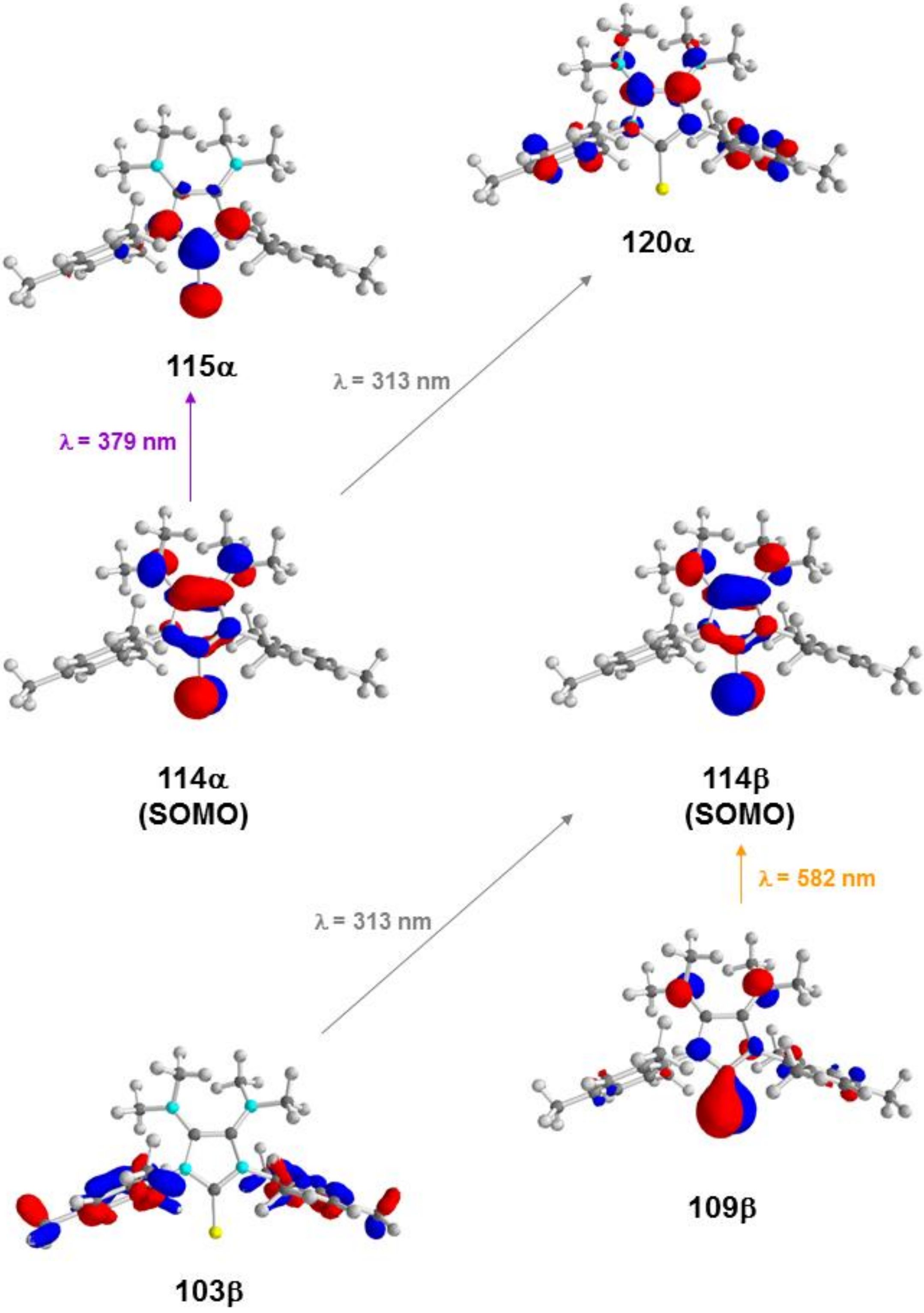

Figure S4. Depiction of the orbitals involved in the major transitions corresponding to the absorption UV-Vis spectrum of $[\mathbf{1}^{(\mathrm{NMe_2})_2}]^{\bullet+}$. Iso-density value: 0.05 a.u.

Computation of ^{13}C NMR screening constants for dicationic [$1^{(NMe_2)_2}$]$^{2+}$

For NMR computations, geometry optimizations of all species were performed in acetonitrile ($\varepsilon = 37.5$). NMR screening constants have been computed using the SAOP (Statistical Average of Orbital Potentials)[14] exchange-correlation potential particularly suitable for modeling NMR quantities. In addition to using TZ2P basis sets (see above), attempts to better the computation of NMR screening constants using quadrupole-zeta (QZ4P) basis sets did not significantly improve the results and are therefore not presented here.

Results

 # ADF labels

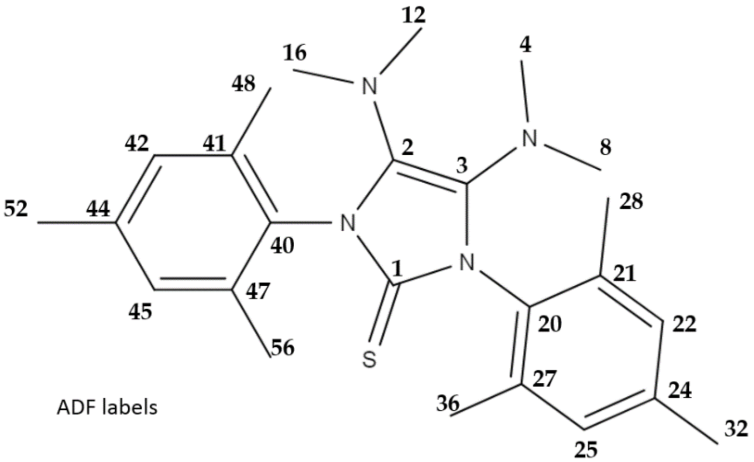

#	Exp (δ)	DFT (σ)	average	δ via Eq.1	Δδ²	δ via Eq.2	Δδ²
1	170.7	17.2	17.2	163.74	48.47	162.97	59.68
2	155.2	26.5	26.4	154.60	0.35	154.00	1.44
3	155.2	26.3	26.4	154.80	0.16	154.00	1.44
4	51	132.6	132.6	50.40	0.36	50.43	0.33
8	48.1	135.8	135.8	47.26	0.70	47.30	0.63
12	51	132.7	132.7	50.31	0.48	50.33	0.45
16	48.1	135.9	135.9	47.16	0.88	47.21	0.80
20	129.8	50.5	50.5	131.03	1.52	130.50	0.49
21	137.3	42.9	43.1	138.50	1.43	137.71	0.17
22	131.3	50.9	50.7	130.64	0.43	130.30	1.00
24	144.6	34	34	147.24	6.96	146.59	3.96
25	131.3	50.6	50.7	130.94	0.13	130.30	1.00
27	137.3	43.3	43.1	138.11	0.65	137.71	0.17
28	18.5	165.2	165	18.39	0.01	18.83	0.11
32	21.2	162	162	21.53	0.11	21.75	0.30
36	18.5	164.7	165	18.88	0.14	18.83	0.11
40	129.8	50.5	50.5	131.03	1.52	130.50	0.49
41	137.3	43.3	43.1	138.11	0.65	137.71	0.17

---

[14] (a) O. V. Gritsenko, P. R. T. Schipper, E. J. Baerends, *Chem. Phys. Lett.* **1999**, *302*, 199; (b) P. R. T. Schipper, O. V. Gritsenko, S. J. A. van Gisbergen, E. J. Baerends, *J. Chem. Phys.* **2000**, 112, 1344.

42	131.3	50.5	50.7	131.03	0.07	130.30	1.00
44	144.6	34.1	34	147.14	6.45	146.59	3.96
45	131.3	50.9	50.7	130.64	0.43	130.30	1.00
47	137.3	43	43.1	138.40	1.21	137.71	0.17
48	18.5	164.7	165	18.88	0.14	18.83	0.11
52	21.2	162.1	162	21.43	0.05	21.75	0.30
56	18.5	165.2	165	18.39	0.01	18.83	0.11

Ideally: $\delta(\text{exp}) = -1.0.\sigma(\text{DFT}) + \sigma(^{13}\text{C\_TMS})$

Eq.1: $\delta(\text{exp}) = -0.9821.\sigma(\text{DFT}) + 180.63$ (includes all 25 carbon nuclei)

→ RMS = 1.7 ppm (1.1 ppm when excluding the first $N_2C{=}S$ carbon: **blue point**)

Eq.2: $\delta(\text{exp}) = -0.9753.\sigma(\text{DFT}) + 179.75$ (includes all - but the first $N_2C{=}S$ - carbon nuclei)

→ RMS = 0.9 ppm

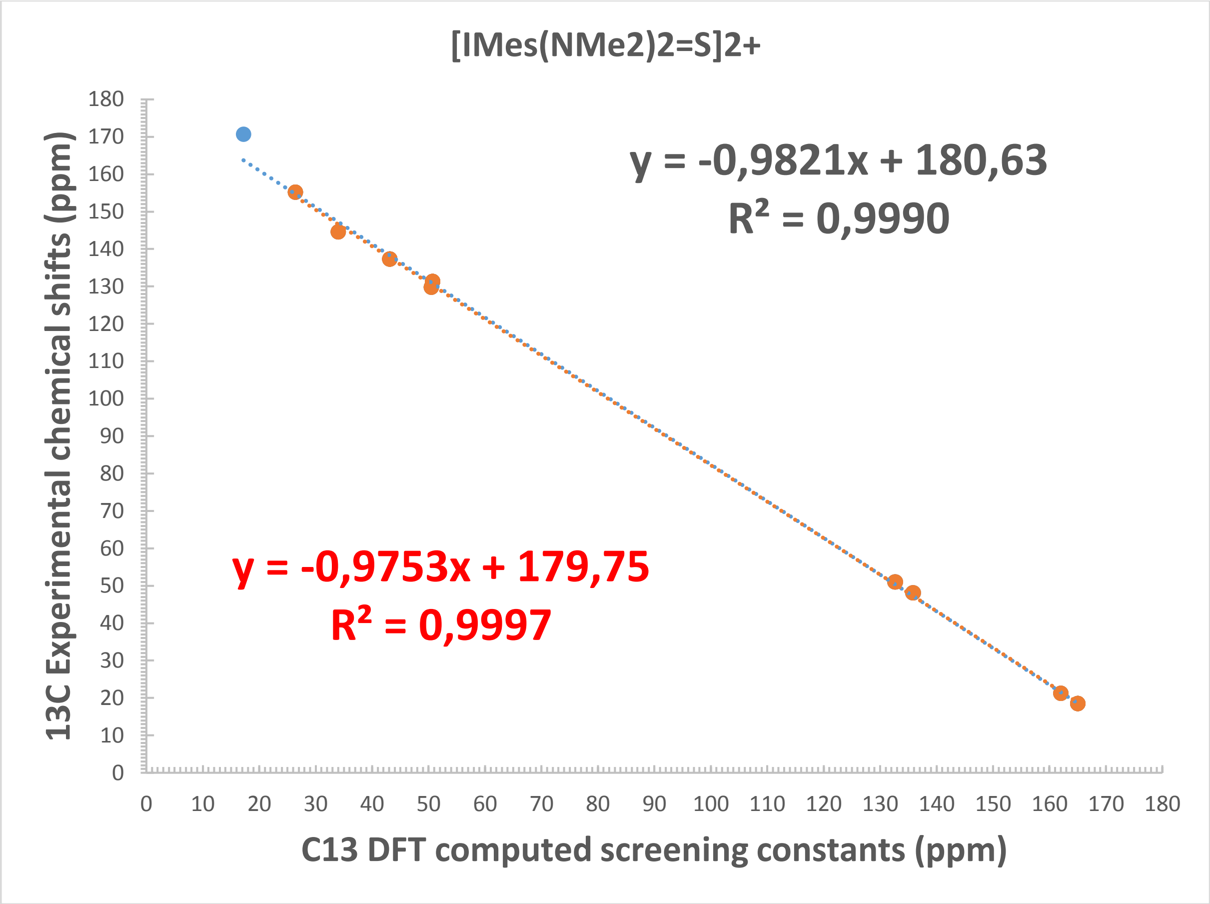

Method: DFT (SCM-ADF code), based on previously optimized geometries (VBP (gga) exchange-correlation potential, TZ2P basis sets), restart with NMR-dedicated SAOP exchange-correlation potential, with TZ2P basis sets.

Using a more extended/flexible basis set (QZ4P) only marginally improved the above results which are therefore not presented. Notice that DFT computation of NMR screening constants are formally performed at 0 K and do not take into account any thermal effects on geometrical structures that may arise for species spectroscopically measured at room temperature.

Technical notes:

→ TZ2P: triple zeta + 2 polarization functions

QZ4P: quadruple zeta + 4 polarization functions

→ “triple zeta” means that each atomic basis (radial part) is a linear combination of 3 exponential decays (4 for “quadruple zeta”).

Additional “polarization functions” to better describe local (i.e. around nuclei) electronic density anisotropies (i.e. beyond first order spherical).

DFT geometry-optimized coordinates

$[\mathbf{1}^{\mathbf{NMe_2}}]^{\bullet+}$

C	4.022543	3.120597	12.042079
C	4.775087	1.262600	13.139191
C	3.394603	1.428181	13.397704
C	4.921254	-0.667351	14.588480
H	5.725483	-1.128306	15.168171
H	4.373271	-1.452987	14.050622
H	4.248485	-0.147963	15.276095
C	6.891280	-0.080337	13.217305
H	7.254427	0.585022	12.434419
H	6.877689	-1.113472	12.844914
H	7.561787	-0.031543	14.084965
C	6.448809	2.648289	11.778240
C	7.312273	3.412279	12.581204
C	8.564972	3.740696	12.049413
H	9.248445	4.336089	12.656518
C	8.956321	3.338118	10.765893
C	8.053528	2.588996	9.998833
H	8.335733	2.275017	8.992827
C	6.789359	2.230748	10.479963
C	6.916907	3.877033	13.959122
H	7.717294	4.475027	14.406669
H	6.712883	3.034167	14.635557
H	6.009425	4.496951	13.926910
C	10.321491	3.686474	10.229269
H	11.040543	2.883618	10.451298
H	10.706887	4.606008	10.685122
H	10.302017	3.813073	9.140138
C	5.841780	1.427234	9.628402
H	4.934773	2.002747	9.393536

H	5.521003	0.503375	10.130570
H	6.317558	1.147233	8.683087
C	1.600278	3.006669	12.763053
C	1.210699	3.866880	13.801903
C	-0.130754	4.269723	13.831167
H	-0.454187	4.942041	14.626990
C	-1.058221	3.836492	12.875919
C	-0.615962	2.980279	11.857813
H	-1.322223	2.635869	11.100807
C	0.711363	2.545081	11.777093
C	2.183236	4.352626	14.845783
H	2.616532	3.520541	15.419049
H	1.682334	5.019785	15.554441
H	3.015958	4.906756	14.389815
C	-2.504029	4.257869	12.951882
H	-3.119802	3.449006	13.372656
H	-2.906182	4.483673	11.956275
H	-2.631527	5.139032	13.590735
C	1.154177	1.620797	10.672202
H	0.308335	1.362773	10.026909
H	1.573362	0.684532	11.067490
H	1.927125	2.088478	10.045775
S	3.957144	4.496168	11.127827
N	5.137526	2.309703	12.297401
N	2.969348	2.531647	12.737260
N	5.534380	0.276832	13.640428
H	2.721099	0.812815	13.977338

1$^{(NMe_2)_2}$

C	3.964882	3.139324	12.091466
C	4.745413	1.235881	13.108920
C	3.384467	1.286937	13.315997
C	5.676077	0.012083	15.005257
H	6.683757	-0.273280	15.339797
H	5.004381	-0.843313	15.202048
H	5.340186	0.864845	15.605928
C	6.255445	-0.664616	12.719103
H	6.430678	-0.272672	11.711485
H	5.571096	-1.530571	12.648711
H	7.215775	-1.018198	13.117528
C	2.631446	-1.025949	13.535180
H	2.919944	-1.126473	12.482803
H	1.663944	-1.527874	13.679747
H	3.377479	-1.553589	14.156918
C	2.017845	0.619411	15.248295
H	1.091168	0.052839	15.410998
H	1.798027	1.681374	15.400992
H	2.756086	0.298473	16.006792
C	6.396167	2.681058	11.832857
C	7.303341	3.334528	12.684565

C	8.583843	3.616152	12.190337
H	9.293125	4.131565	12.840710
C	8.971839	3.265647	10.890250
C	8.033554	2.625719	10.069968
H	8.308674	2.358128	9.048007
C	6.740030	2.323866	10.516780
C	6.914167	3.744430	14.080897
H	7.725188	4.301789	14.562457
H	6.684913	2.866348	14.700461
H	6.016123	4.378350	14.073316
C	10.368123	3.552899	10.393911
H	11.040724	2.709219	10.611144
H	10.791566	4.439223	10.881858
H	10.383193	3.708522	9.308293
C	5.746971	1.670018	9.590414
H	4.910673	2.353095	9.378782
H	5.311709	0.760358	10.026740
H	6.221482	1.399538	8.640834
C	1.567302	2.957869	12.727670
C	1.190551	3.917965	13.682141
C	-0.142831	4.352548	13.687460
H	-0.445667	5.100264	14.422849
C	-1.087271	3.860970	12.778379
C	-0.666403	2.913491	11.834266
H	-1.381556	2.528737	11.104515
C	0.653041	2.446866	11.788893
C	2.185727	4.504560	14.650174
H	2.760367	3.729437	15.175036
H	1.680803	5.123831	15.399575
H	2.915067	5.132603	14.116380
C	-2.523170	4.324534	12.820035
H	-3.161322	3.577702	13.315858
H	-2.925565	4.469006	11.809178
H	-2.624118	5.265177	13.373951
C	1.075045	1.442905	10.748045
H	0.251107	1.228564	10.058462
H	1.387063	0.498370	11.215062
H	1.928913	1.811929	10.162475
S	3.887481	4.600444	11.225273
N	5.077438	2.371495	12.321105
N	2.927833	2.487228	12.706385
N	5.740906	0.393774	13.593891
N	2.481396	0.389235	13.876394

$[1^{(\mathrm{NMe}_2)_2}]^{\bullet+}$

C	3.968848	3.072554	12.131223
C	4.761220	1.153171	13.083976
C	3.373480	1.270700	13.403364
C	5.572511	-0.296402	14.897768
H	6.517401	-0.050581	15.403569

H	5.453702	-1.387289	14.897840
H	4.750694	0.166356	15.448489
C	6.800365	-0.236123	12.759407
H	6.656099	-0.061422	11.691186
H	6.905540	-1.315855	12.927707
H	7.721769	0.261531	13.094852
C	2.759414	-1.068669	13.847864
H	3.567505	-1.270820	13.141489
H	1.822365	-1.469035	13.434345
H	2.961100	-1.575495	14.799927
C	1.437538	0.742202	14.875681
H	0.494545	0.606062	14.326636
H	1.516179	1.775671	15.219441
H	1.430468	0.080252	15.751554
C	6.386479	2.607200	11.779093
C	7.271090	3.260306	12.654456
C	8.531353	3.613618	12.156659
H	9.228022	4.126914	12.821361
C	8.912620	3.341613	10.836604
C	7.988798	2.705653	9.996546
H	8.260287	2.498552	8.960179
C	6.716313	2.329481	10.441677
C	6.888163	3.602243	14.071710
H	7.680566	4.184838	14.552859
H	6.720533	2.702844	14.681724
H	5.963669	4.196239	14.104199
C	10.287035	3.710577	10.337194
H	10.993949	2.883324	10.501253
H	10.682463	4.586113	10.865850
H	10.278275	3.922525	9.261398
C	5.742244	1.667140	9.502755
H	4.883147	2.325003	9.305822
H	5.342175	0.728925	9.912615
H	6.222640	1.439007	8.545710
C	1.580685	2.974284	12.818639
C	1.210715	3.992505	13.711849
C	-0.108148	4.460333	13.651812
H	-0.412235	5.251782	14.338441
C	-1.037352	3.948502	12.738013
C	-0.616132	2.944941	11.854623
H	-1.318744	2.544948	11.121649
C	0.689165	2.441043	11.870397
C	2.187845	4.583894	14.693793
H	2.675360	3.815071	15.309974
H	1.683075	5.284736	15.366607
H	2.985750	5.128633	14.168208
C	-2.457692	4.454705	12.706302
H	-3.141079	3.725600	13.166125
H	-2.801640	4.609792	11.675569
H	-2.558989	5.398424	13.253955
C	1.111704	1.385877	10.880224

H	0.292173	1.155687	10.191644
H	1.403456	0.448306	11.374867
H	1.971578	1.721139	10.282626
S	3.893505	4.495970	11.280050
N	5.073104	2.236739	12.267204
N	2.940378	2.473853	12.852505
N	5.633732	0.216071	13.522888
N	2.596741	0.375473	14.056764

$[1^{(NMe_2)_2}]^{2+}$

C	3.973543	3.029667	12.164502
C	4.804938	1.140581	13.130269
C	3.331913	1.219915	13.391384
C	5.428084	-0.326177	15.000943
H	6.296307	-0.066175	15.618045
H	5.385598	-1.414245	14.896870
H	4.527407	0.063729	15.474324
C	7.021227	0.044581	13.165862
H	7.059656	0.187202	12.086326
H	7.246933	-0.997880	13.410900
H	7.748157	0.693986	13.668685
C	2.899274	-1.165637	13.793832
H	3.784387	-1.326754	13.178673
H	2.038107	-1.641571	13.309667
H	3.022478	-1.598253	14.790859
C	1.216927	0.501277	14.453072
H	0.453604	0.293895	13.692968
H	1.118119	1.518836	14.829462
H	1.100221	-0.211313	15.276066
C	6.391198	2.578092	11.759732
C	7.240174	3.356470	12.563464
C	8.467571	3.735195	12.008023
H	9.145720	4.339676	12.611615
C	8.842221	3.368878	10.708305
C	7.946974	2.606883	9.944773
H	8.216593	2.320610	8.927471
C	6.706228	2.197977	10.444905
C	6.860968	3.789724	13.955772
H	7.664577	4.381189	14.404846
H	6.671685	2.936594	14.623484
H	5.954324	4.412017	13.950826
C	10.184058	3.768520	10.151486
H	10.936479	2.996755	10.372955
H	10.537995	4.705761	10.596352
H	10.146113	3.883307	9.061930
C	5.761579	1.385491	9.598933
H	4.833569	1.938397	9.393868
H	5.479328	0.439807	10.083715
H	6.222947	1.139467	8.637786
C	1.579252	2.979847	12.857690

C	1.228350	3.934125	13.825242
C	-0.065804	4.463315	13.756441
H	-0.365002	5.202029	14.500723
C	-0.977109	4.073222	12.766684
C	-0.565985	3.129413	11.814418
H	-1.257117	2.821633	11.028625
C	0.713537	2.565335	11.830938
C	2.188093	4.377770	14.897583
H	2.571898	3.532382	15.486544
H	1.696507	5.067794	15.589937
H	3.055517	4.897308	14.465554
C	-2.372250	4.641475	12.729831
H	-3.097986	3.907016	13.109099
H	-2.673399	4.888004	11.703836
H	-2.454246	5.542471	13.347586
C	1.129870	1.574616	10.775044
H	0.302002	1.378928	10.086904
H	1.434628	0.608414	11.202622
H	1.973975	1.952875	10.180085
S	3.900660	4.422765	11.336125
N	5.094355	2.179249	12.291851
N	2.927584	2.428211	12.900406
N	5.662258	0.302966	13.685567
N	2.566321	0.269455	13.897831

NMR Spectra

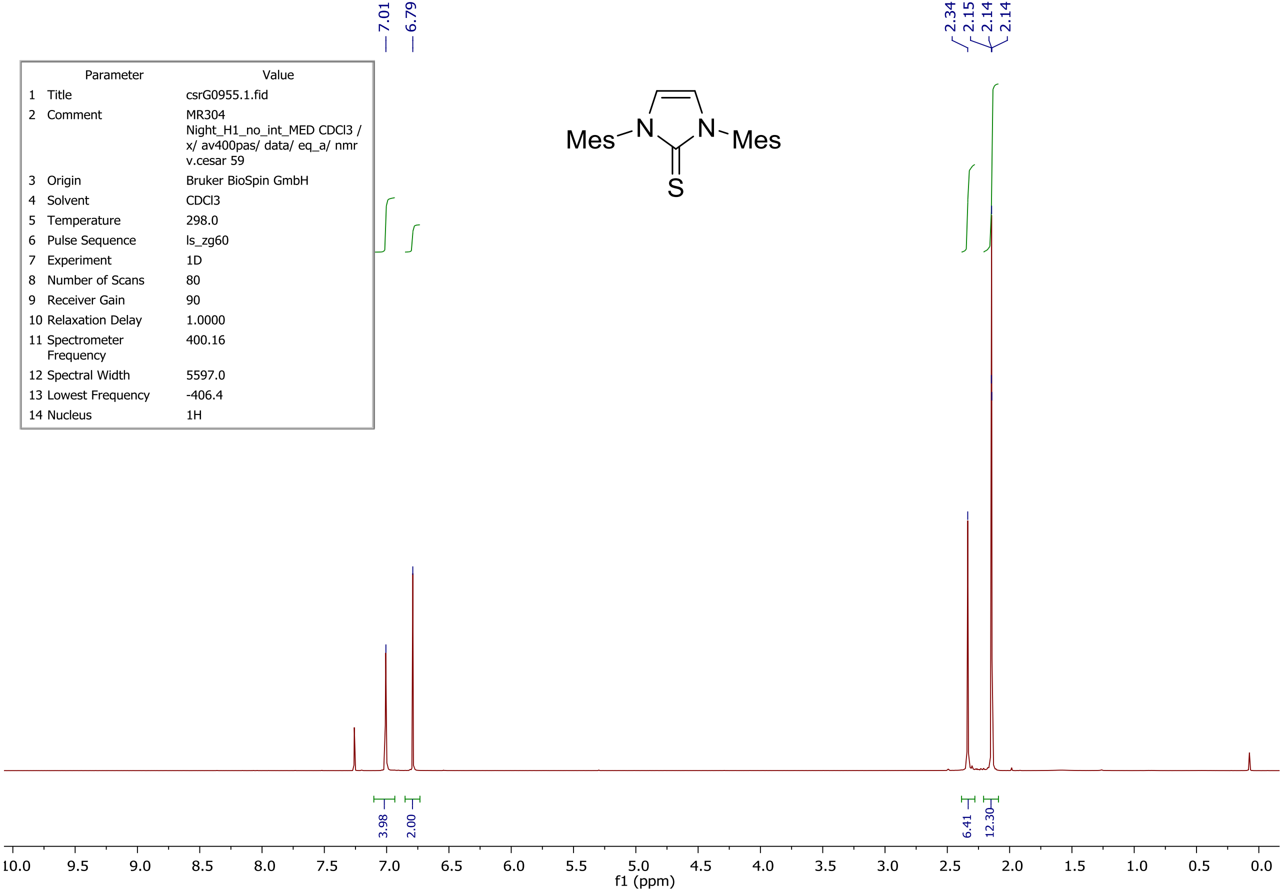

	Parameter	Value
1	Title	csrG0955.1.fid
2	Comment	MR304 Night_H1_no_int_MED CDCl3 / x/ av400pas/ data/ eq_a/ nmr v.cesar 59
3	Origin	Bruker BioSpin GmbH
4	Solvent	CDCl3
5	Temperature	298.0
6	Pulse Sequence	ls_zg60
7	Experiment	1D
8	Number of Scans	80
9	Receiver Gain	90
10	Relaxation Delay	1.0000
11	Spectrometer Frequency	400.16
12	Spectral Width	5597.0
13	Lowest Frequency	-406.4
14	Nucleus	1H

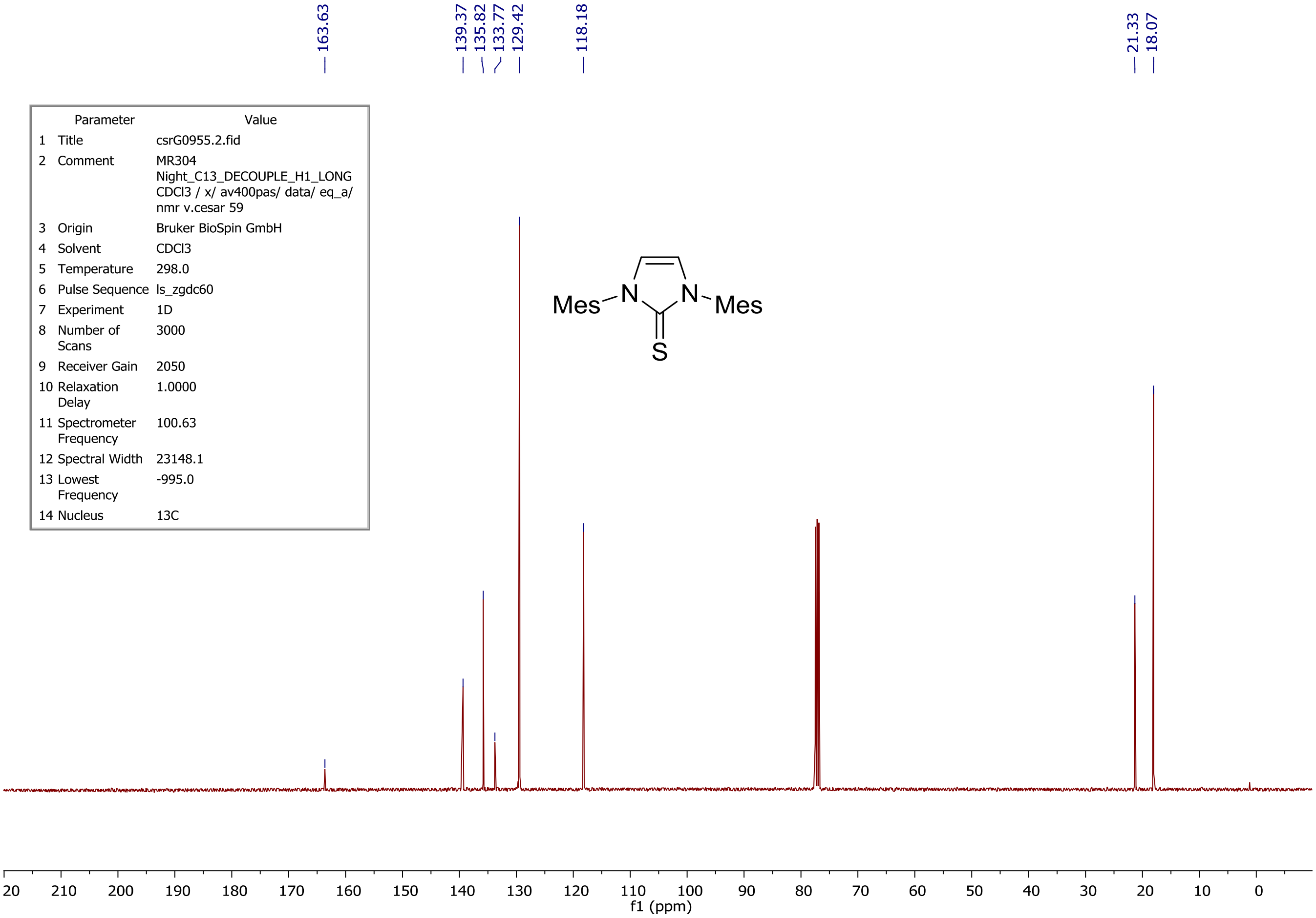

	Parameter	Value
1	Title	csrG0955.2.fid
2	Comment	MR304 Night_C13_DECOUPLE_H1_LONG CDCl3 / x/ av400pas/ data/ eq_a/ nmr v.cesar 59
3	Origin	Bruker BioSpin GmbH
4	Solvent	CDCl3
5	Temperature	298.0
6	Pulse Sequence	ls_zgdc60
7	Experiment	1D
8	Number of Scans	3000
9	Receiver Gain	2050
10	Relaxation Delay	1.0000
11	Spectrometer Frequency	100.63
12	Spectral Width	23148.1
13	Lowest Frequency	-995.0
14	Nucleus	13C

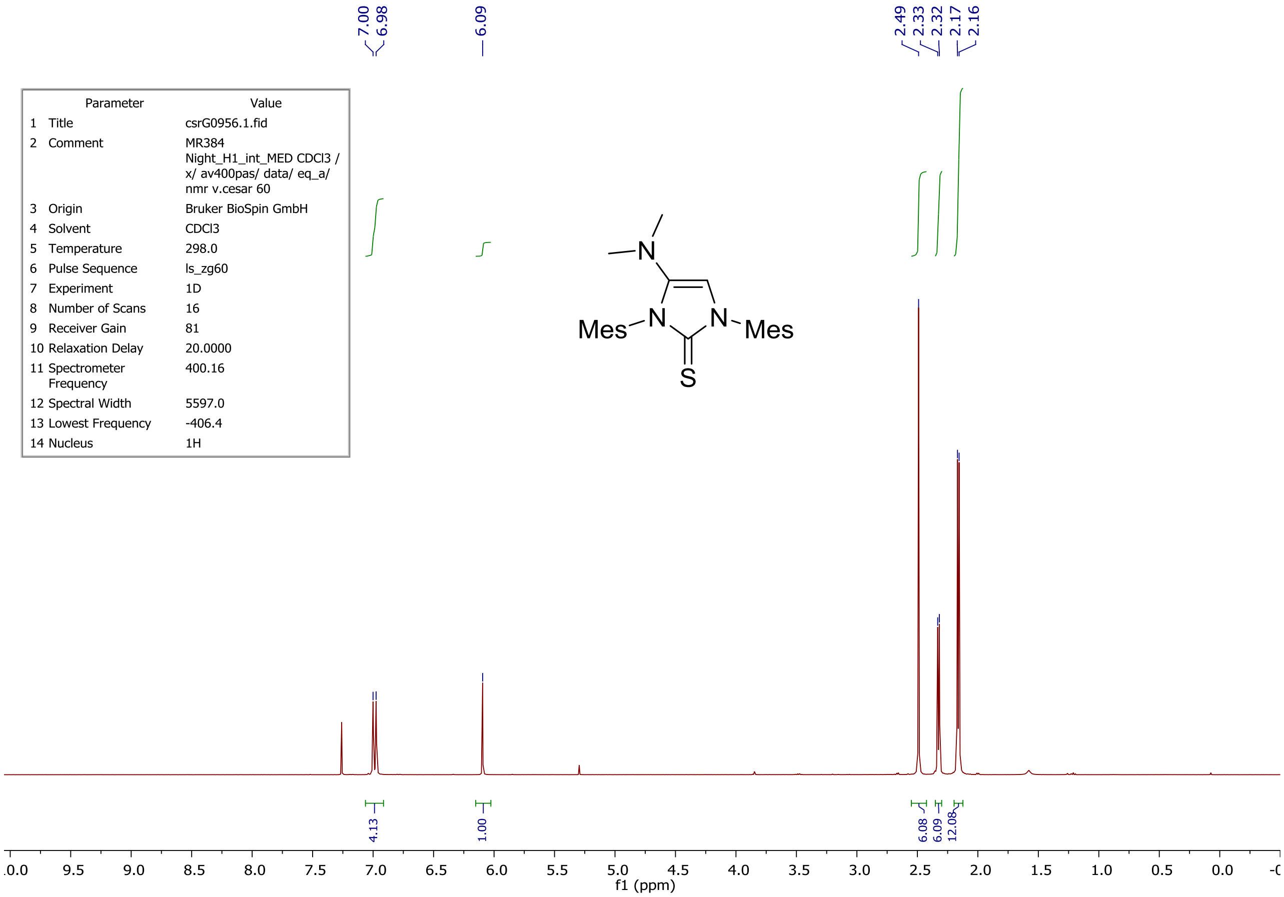

Parameter	Value
1 Title	csrG0956.1.fid
2 Comment	MR384 Night_H1_int_MED CDCl3 / x/ av400pas/ data/ eq_a/ nmr v.cesar 60
3 Origin	Bruker BioSpin GmbH
4 Solvent	CDCl3
5 Temperature	298.0
6 Pulse Sequence	ls_zg60
7 Experiment	1D
8 Number of Scans	16
9 Receiver Gain	81
10 Relaxation Delay	20.0000
11 Spectrometer Frequency	400.16
12 Spectral Width	5597.0
13 Lowest Frequency	-406.4
14 Nucleus	1H

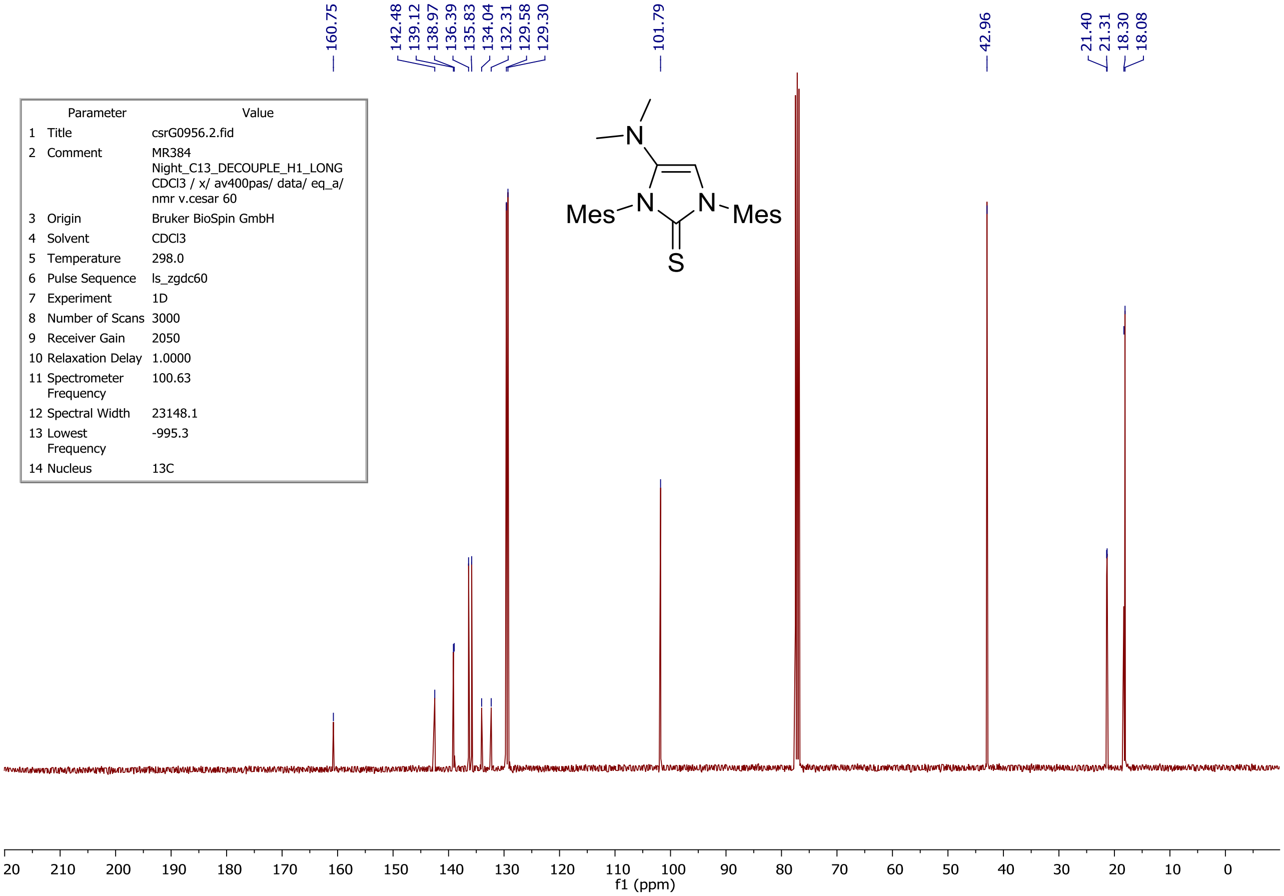

Parameter	Value
1 Title	csrG0956.2.fid
2 Comment	MR384 Night_C13_DECOUPLE_H1_LONG CDCl3 / x/ av400pas/ data/ eq_a/ nmr v.cesar 60
3 Origin	Bruker BioSpin GmbH
4 Solvent	CDCl3
5 Temperature	298.0
6 Pulse Sequence	ls_zgdc60
7 Experiment	1D
8 Number of Scans	3000
9 Receiver Gain	2050
10 Relaxation Delay	1.0000
11 Spectrometer Frequency	100.63
12 Spectral Width	23148.1
13 Lowest Frequency	-995.3
14 Nucleus	13C

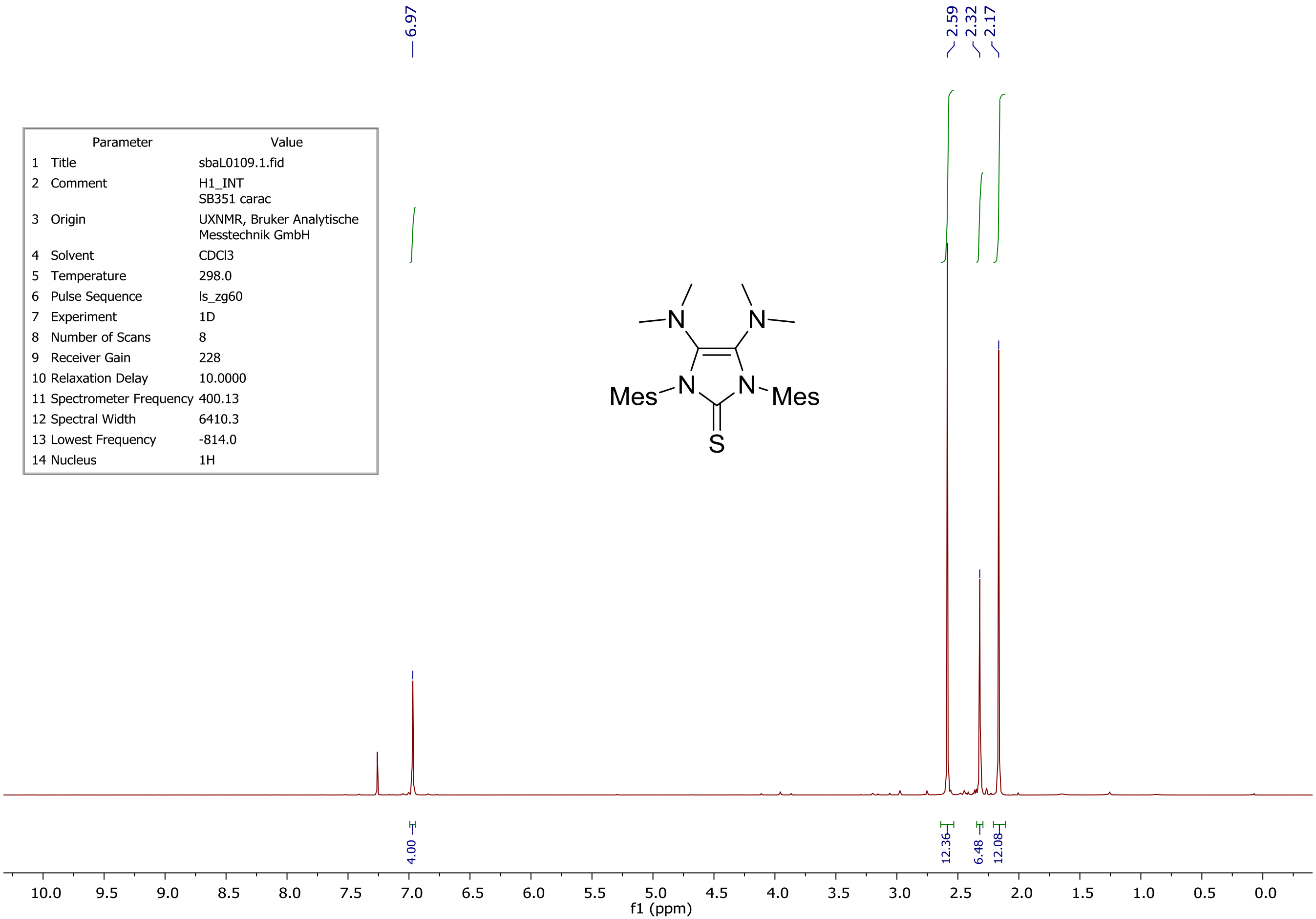

	Parameter	Value
1	Title	sbaL0109.1.fid
2	Comment	H1_INT SB351 carac
3	Origin	UXNMR, Bruker Analytische Messtechnik GmbH
4	Solvent	CDCl3
5	Temperature	298.0
6	Pulse Sequence	ls_zg60
7	Experiment	1D
8	Number of Scans	8
9	Receiver Gain	228
10	Relaxation Delay	10.0000
11	Spectrometer Frequency	400.13
12	Spectral Width	6410.3
13	Lowest Frequency	-814.0
14	Nucleus	1H

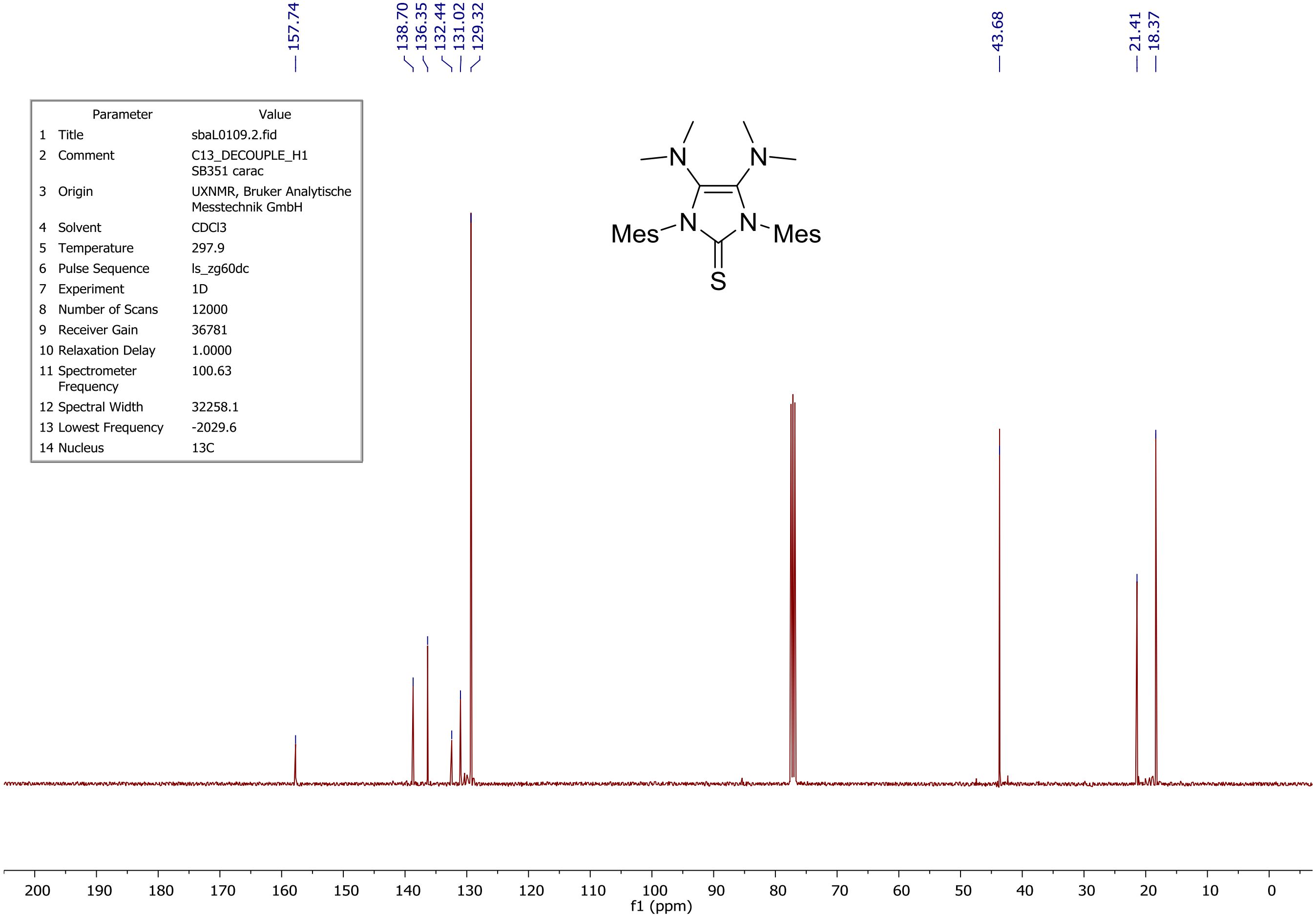

	Parameter	Value
1	Title	sbaL0109.2.fid
2	Comment	C13_DECOUPLE_H1 SB351 carac
3	Origin	UXNMR, Bruker Analytische Messtechnik GmbH
4	Solvent	CDCl3
5	Temperature	297.9
6	Pulse Sequence	ls_zg60dc
7	Experiment	1D
8	Number of Scans	12000
9	Receiver Gain	36781
10	Relaxation Delay	1.0000
11	Spectrometer Frequency	100.63
12	Spectral Width	32258.1
13	Lowest Frequency	-2029.6
14	Nucleus	13C

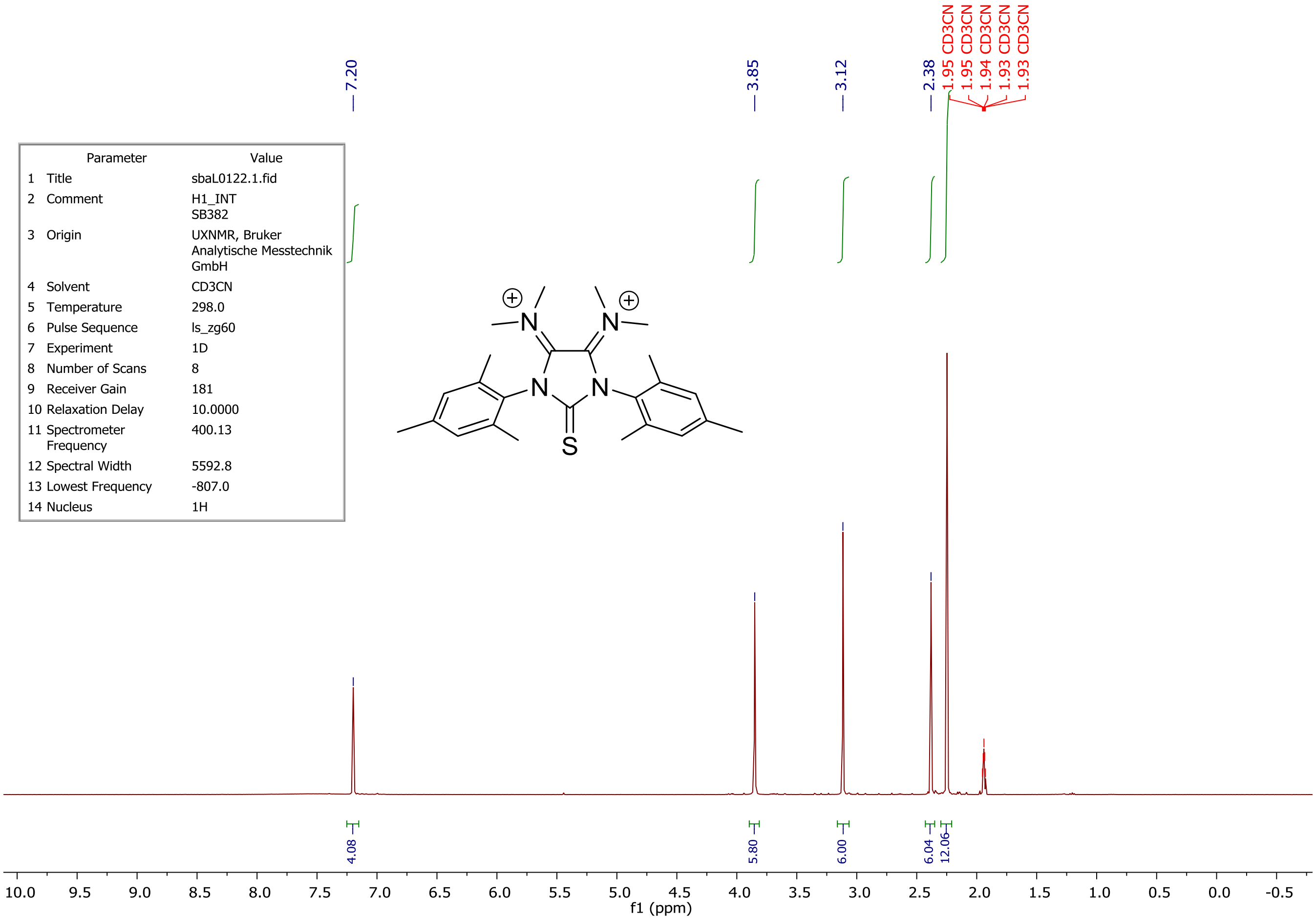

	Parameter	Value
1	Title	sbaL0122.1.fid
2	Comment	H1_INT SB382
3	Origin	UXNMR, Bruker Analytische Messtechnik GmbH
4	Solvent	CD3CN
5	Temperature	298.0
6	Pulse Sequence	ls_zg60
7	Experiment	1D
8	Number of Scans	8
9	Receiver Gain	181
10	Relaxation Delay	10.0000
11	Spectrometer Frequency	400.13
12	Spectral Width	5592.8
13	Lowest Frequency	-807.0
14	Nucleus	1H

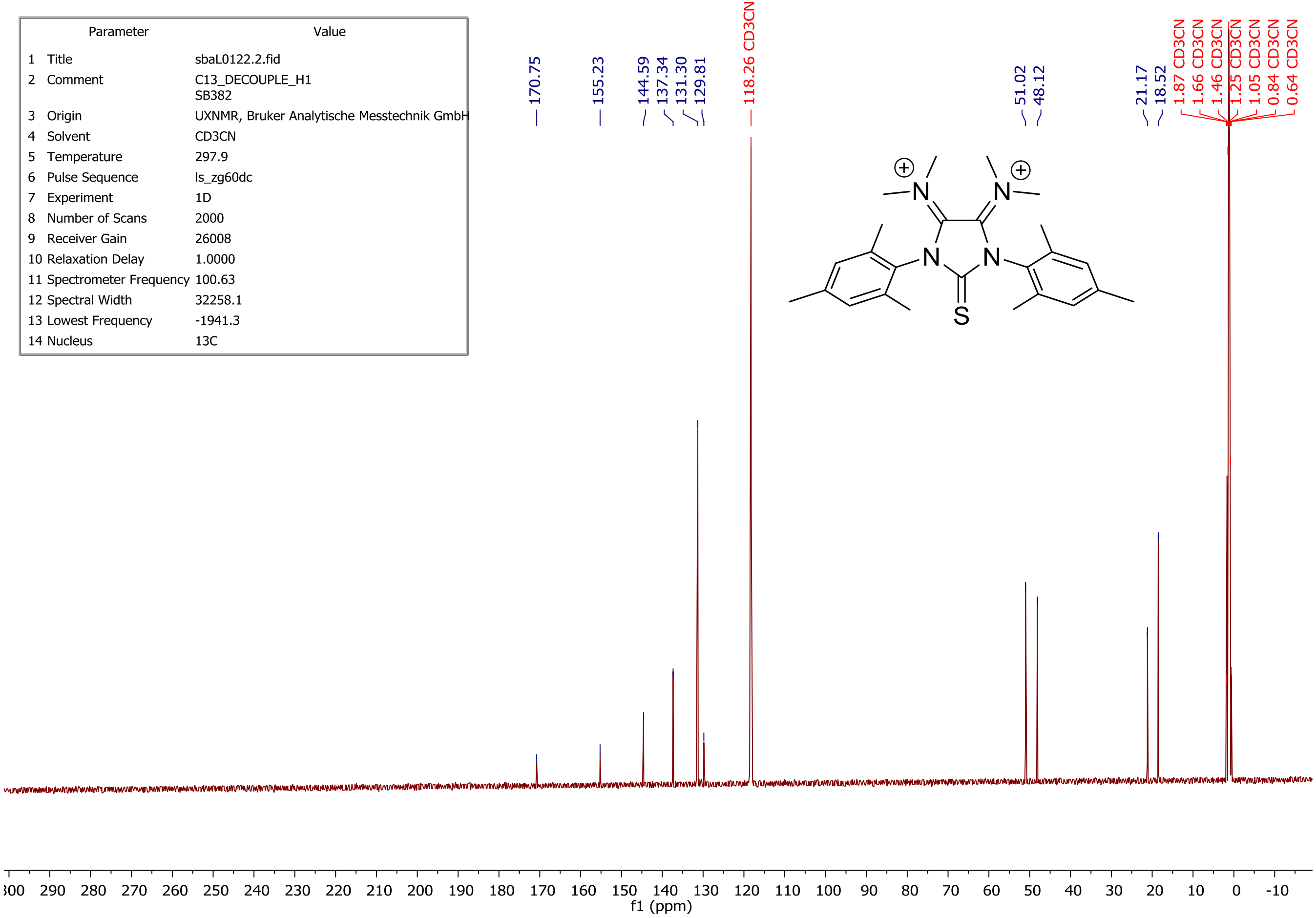

	Parameter	Value
1	Title	sbaL0122.2.fid
2	Comment	C13_DECOUPLE_H1 SB382
3	Origin	UXNMR, Bruker Analytische Messtechnik GmbH
4	Solvent	CD3CN
5	Temperature	297.9
6	Pulse Sequence	ls_zg60dc
7	Experiment	1D
8	Number of Scans	2000
9	Receiver Gain	26008
10	Relaxation Delay	1.0000
11	Spectrometer Frequency	100.63
12	Spectral Width	32258.1
13	Lowest Frequency	-1941.3
14	Nucleus	13C